

A Geometric Analysis-Based Safety Assessment Framework for MASS Route Decision-Making in Restricted Waters

Zilong Xu, Zihao Wang, *Member, IEEE*, He Li, *Member, IEEE*, Dingli Yu, Zaili Yang, Jin Wang

Abstract—To enhance the safety of Maritime Autonomous Surface Ships (MASS) navigating in restricted waters, this paper aims to develop a geometric analysis-based route safety assessment (GARSA) framework, specifically designed for their route decision-making in irregularly shaped waterways. Utilizing line and point geometric elements to define waterway boundaries, the framework enables to construct a dynamic width characterization function to quantify spatial safety along intricate waterways. An iterative method is developed to calculate this function, enabling an abstracted spatial property representation of the waterways. Based on this, we introduce a navigational safety index that balances global navigational safety and local risk to determine the safest route. To accommodate ship kinematic constraints, path modifications are applied using a dynamic window approach. A case study in a simulated Port of Hamburg environment shows that GARSA effectively identifies safe routes and avoids the risk of entering narrow waterways in an autonomous manner, thereby prioritizing safety in route decision-making for MASS in confined waters.

Index Terms—Intelligent transportation system, autonomous navigation, navigation safety assessment, autonomous ship.

I. INTRODUCTION

MARITIME transportation is undergoing a transformative shift with the introduction of Maritime Autonomous Surface Ships (MASS). These vessels enable autonomous navigation and operations in complex environments without direct human intervention [1], driven by advancements in automation, robotics, multi-sensor perception, and intelligent decision-making concepts [2], [3]. Among the diverse operational environments, restricted waters, such as ports and intricate waterways, pose significant challenges for MASS due to their narrow and irregular geometries, which require precise maneuvering and advanced decision-making [4].

One of the cores for MASS operating in restricted waters is ensuring safe navigation in an autonomous manner [5]–[7]. The autonomous control framework typically operates on two hierarchical levels: (i) a high-level decision-making layer, responsible for identifying feasible routes and selecting the optimal route based on performance evaluations [8], [9]; and

(ii) a low-level motion control layer, tasked with executing the planned route to achieve precise vessel maneuvering [10], [11].

In typical navigation scenarios in restricted waters, such as entering and exiting ports or traversing rugged waterways, route decision-making plays a critical role in mitigating collision risks. Effective route planning enables vessels to avoid excessively narrow or rugged sections, thereby reducing the likelihood of collisions and minimizing transportation disruptions. This task relies heavily on understanding the irregular geometry of waterways and assessing the safety properties of navigational paths. Specifically, it addresses two key aspects: (i) route network modeling, which identifies navigational pathways between decision points, and (ii) safety assessment and route selection, which evaluates routes based on safety criteria and determines the safest path.

Route network modeling refers to constructing an abstract representation of intricate waterways to capture the topological structure within a specific environment. In localized environments, this differs significantly from global route network modeling, which leverages abundant Automatic Identification System (AIS) data [12], [13] and advanced techniques such as Bayesian analysis [14]. Localized route network modeling often lacks sufficient navigational data and requires tailored approaches. Common methods involve selecting key nodes and connecting them if the line between two nearest nodes within feasible regions. For instance, Jang et al. [15] used a random generation method to obtain nodes in feasible regions. However, this method may generate redundant nodes in complex waterways. Zhou et al. [16] connected boundary elements of polygonal obstacles to construct the network, while Shah et al. [17] simplified networks by removing redundant nodes. Additionally, Schoener et al. [18] utilized Voronoi diagrams to divide waterways into regions, deriving central axes as potential pathways. These methods effectively capture connectivity but generally focus on distance attributes, with limited integration of safety metrics, especially in intricate waterways. To enhance safety assessment, integrating safety-related evaluation metrics into the network model is essential.

In constrained waterways, navigational safety is often addressed through path planning. One category of strategies focuses on maintaining safe distances from obstacles [19]. Singh et al. [20] enhanced the A* algorithm by introducing circular safety zones, with the radius determined by balancing the unmanned surface vehicle’s maneuverability and computational efficiency. Han et al. [21] developed a risk cost function

This work was supported in part by the National Natural Science Foundations of China under Grant 52101361.

Corresponding authors: zihao wang@shu.edu.cn

Z. Xu and Z. Wang are with the Institute of Artificial Intelligence, Shanghai University, and the Engineering Research Center of Unmanned Intelligent Marine Equipment, Ministry of Education, Shanghai, China (e-mail: zlong_xu@163.com, zihao wang@shu.edu.cn). H. Li, D. Yu, and Z. Yang, J. Wang are with the School of Engineering, Liverpool John Moores University, Liverpool, UK (e-mail: h.li@ljmu.ac.uk, d.yu@ljmu.ac.uk, z.yang@ljmu.ac.uk, j.wang@ljmu.ac.uk).

for the NT* algorithm to prevent vessels from approaching shores, which is based on the distance between navigational cells and obstacles. Another category considers the vessel's kinematic constraints. Song et al. [22] designed a cubic spline-based smoother to refine jagged paths, while Han et al. [23] combined the Dynamic Window Approach (DWA) with physical models to account for dynamic constraints during autonomous berthing. Furthermore, some studies have utilized AIS data to predict ship trajectories, reflecting the kinematic characteristics of ships and reducing the risk of collisions [24], [25]. Some researchers have integrated these strategies to further improve safety. For example, Zhao et al. [26] presented a Genetic Algorithm with an objective function integrating safe distance and path smoothness. Liu et al. [27] proposed a risk model for the A* algorithm, ensuring a balance between collision risk and kinematic constraints. Wang et al. [28] employed reinforcement learning for path planning, setting safe distance thresholds and smoothing paths with Bezier curves.

Although these methods improve ship safety during path planning, they primarily treat safety as a secondary factor to path length optimization. In complex waterways, such approaches are insufficient for comprehensive safety evaluations. Existing studies generally lack a global perspective that prioritizes safety as the central criterion. This gap highlights the necessity for route safety assessments in constrained waterways, integrating safety evaluations into the routing process to comprehensively address navigational risks in complex environments.

To prioritize safety in route decision-making for irregularly shaped waterways, this research aims to develop a geometric analysis-based route safety assessment (GARSA) framework that can address both route exploration and quantitative safety assessment. Safety concerns are considered from the perspective of a potential navigable space. To capture spatial variations in irregularly shaped waterways, a definition of dynamic width characteristics is presented, which serves as a foundation for assessing navigational safety. An iterative method is proposed to calculate the dynamic width characterization function along the waterway while obtaining an abstracted spatial representation of the environment by analyzing the point and line characteristics of the waterway boundary. Building upon this, a safety performance index is developed to balance global navigational safety and local risk when determining the safest route. Furthermore, the paths are modified using a dynamic window approach to accounting for the vessels' kinematic constraints. Validation in simulated complex waterways (i.e., the Port of Hamburg) is conducted to demonstrate that GARSA efficiently explores feasible routes and considers safety features, providing decision support for selecting safe routes in complex restricted environments.

The structure of this paper is as follows. Section II introduces the dynamic width characterization function. Section III addresses the safety route decision-making process. Section IV presents the simulation experiments and results analysis. Section V concludes the entire work and makes the prospect.

II. DYNAMIC WIDTH CHARACTERIZATION FUNCTION

Under ideal conditions, the navigational safety of a regularly shaped waterway can be assessed based on their width, which reflects the potential risk of collision with the shore to some extent. However, in real-world environments, such as ports and inland rivers, waterways often have irregular boundaries, causing the width to vary dynamically at different locations. To assess the navigational safety of an entire irregularly shaped waterway, we develop a dynamic width characterization function. This function effectively captures the variation in waterway width as ships navigate through irregularly shaped waterways, providing a foundation for assessing navigational safety.

A. Geometric Description for Waterway Boundaries

At first, an irregularly shaped waterway can be viewed as consisting of multiple connected sub-waterway units. The boundaries of these units can be further simplified and represented by point features H_p and line features H_l . It is assumed that the waterway boundaries ensure that the water depth at any point exceeds the potential ship's draft, making the entire area navigable. Fig. 1 illustrates this concept with each waterway composes three connected sub-waterway units. The sub-waterway units can be approximated using combinations of 'line-line', 'point-line', or 'point-point' arrangements. On this basis, the safety assessment of the waterway can be conducted within each sub-waterway unit.

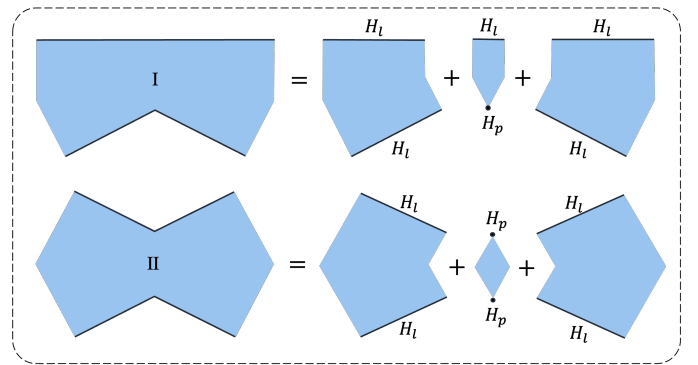


Fig. 1. Decomposition of the Waterway

B. Dynamic Width Characteristic

Definition 1 (*Dynamic width characteristic*). Given point and line features H_i ($i = 1, 2, \dots, n$) decomposed from the waterway boundary, consider a trajectory L , which represents a cross-section at specific positions along the waterway. For any point P_j on this trajectory, define the minimum distance from P_j to all surrounding geometric elements H_i as w_{P_j} :

$$w_{P_j} = \min_{1 \leq i \leq n} \text{dist}(P_j, H_i), \quad (1)$$

where $\text{dist}(P_j, H_i)$ represents the distance between P_j and H_i . Then, $\exists P_q \in L$ such that:

$$w_{P_q} \geq w_{P_j} \quad \text{s.t. } P_j \in L, \quad (2)$$

where $\omega_{dwc} := w_{P_q}$ is defined as the *dynamic width characteristic* of the waterway at the specific location represented by the cross-section L .

To offer an intuitive understanding, the dynamic width characteristic is illustrated with an irregularly shaped waterway shown in Fig. 2. The waterway boundary can be roughly decomposed into three line features, denoted as H_1 , H_2 , and H_3 , and cross-sections L_a , L_b , and L_c with an infinitesimally small width dS are considered. In this context, there exists a point P_d within L_a , where the minimum distance to the surrounding geometric elements, denoted as w_{P_d} , is greater than that at any other point within L_a . Therefore, the dynamic width characteristics of L_a can be determined by P_d as w_{P_d} . Similarly, the dynamic width characteristic of cross-sections L_b and L_c can be determined.

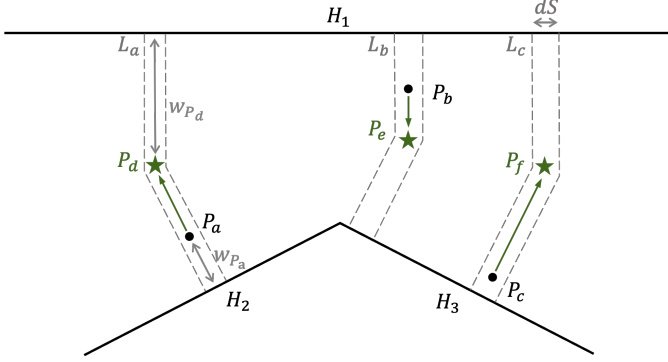


Fig. 2. Illustrative Example of Dynamic Width Characteristic

The approach to determining the waterway cross-sections L can be reflected in the calculation process of the dynamic width characterization function, as detailed in Subsection II-C. Taking L_a as an example, given a point P_a as an initial state, the minimum distance from P_a to all geometric elements is denoted as w_{P_a} , which is related to H_2 . Then, the point is adjusted orthogonally to H_2 until the distance $dist(P_a, H_2)$ equals $dist(P_a, H_1)$; the dynamic width characteristic is obtained at this moment. Meanwhile, the cross-section L_a is generated in this process.

C. Methods for Calculating Dynamic Width Characteristic

1) *Geometric Analysis for Boundary Elements* : As illustrated in the example above, the method for calculating dynamic width characteristics can be intuitively understood as optimizing the position of a object relative to the geometric elements. The foundation of this method is first expressing how the distance changes as an MASS moves relative to point or line features with the geometric boundaries.

A virtual MASS is defined as moving with a constant velocity v in the plane, within its direction governed by the function $\phi(t)$, where $\phi \in [0, 2\pi)$. In the Cartesian coordinate system, the position of the ship $P(t) = [x(t), y(t)]^T$ is subjected to:

$$\frac{dP(t)}{dt} = v \cdot [\cos(\phi(t)), \sin(\phi(t))]^T, \quad (3)$$

where $t = 0$ is set as the initial time and $goal = [x_{end}, y_{end}]^T$ is the destination. The rates of change in distance between the ship and the point or line features are denoted as dD_{H_p}/dt and dD_{H_l}/dt , respectively.

A graphical description of the formal expressions dD_{H_l}/dt and dD_{H_p}/dt is sketched in Fig. 3, with a fixed line feature H_l in Fig. 3 (a) and a fixed point feature H_p in Fig. 3 (b). Assume that within an infinitesimal time interval dt , the ship undergoes a small displacement dP . As the ship moves along different direction angles ϕ , the variation in the distance between the ship and the geometric elements, denoted as ΔD_{H_x} , changes accordingly.

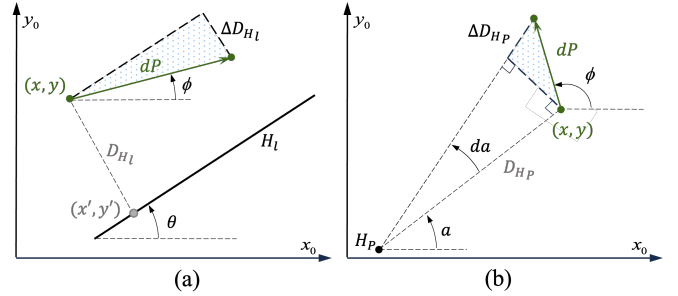


Fig. 3. Illustration of the Relationship between an MASS Movement and Geometric Elements. (a) Line feature. (b) Point feature.

For the line feature H_l , the rate of change in the orthogonal distance dD_{H_l}/dt between the MASS and H_l is given by:

$$\frac{dD_{H_l}}{dt} = \begin{cases} \text{sign}((x - x') \cdot \csc(\theta)) \cdot \sin(\theta - \phi) \cdot v, & \theta \neq 0 \\ \text{sign}(y - y') \cdot \sin(\phi) \cdot v, & \theta = 0 \end{cases}, \quad (4)$$

where $[x', y']^T$ represents the projection coordinates of the object on H_l , and θ denotes the inclination angle of H_l with $\theta \in [0, \pi]$.

For the point feature H_p , a similar approach yields:

$$\frac{dD_{H_p}}{dt} = \cos(\phi - \alpha) \cdot v, \quad (5)$$

where α represents the azimuth angle of the vector from H_p to the object, with $\alpha \in [0, 2\pi)$. After the object moves along the direction angle ϕ by a time step dt , the infinitesimal change in α is given by:

$$d\alpha = \frac{\sin(\phi - \alpha) \cdot v}{D_{H_p}} dt. \quad (6)$$

Based on (4)-(5), the relationship between the ship's movement and its distance to the geometric elements is established, facilitating the calculation of dynamic width characteristic.

2) *Dynamic Width Characterization Function*: Considering that sub-waterway units are categorized as 'line-line', 'point-line', or 'point-point' arrangements, we can calculate the dynamic width characteristics accordingly. Specially, suppose the boundaries of a sub-waterway unit can be decomposed into geometric elements H_1 and H_2 . Without loss of generality, assume the ship's initial position is closer to H_1 . Let the ship move at maximum speed away from H_1 , using (4) or (5) to calculate the direction angle ϕ such that

$dD_{H_i}/dt = v$. Continue this process until the minimum distances to the geometric elements is maximized, thereby obtaining the dynamic width characteristic as defined in **Definition 1**.

Subsequently, continue moving the ship to obtain the dynamic width characteristic at adjacent cross-sections within the sub-waterway unit, calculating the direction angle of the object's movement at each moment, satisfying

$$\frac{dD_{H_1}}{dt} = \frac{dD_{H_2}}{dt}. \quad (7)$$

This allows for the calculation of the dynamic variation in width at different positions within the sub-waterway unit, ultimately yielding the dynamic width characterization function. The dynamic width characterization function can be formalized as

$$\omega_{dwc} = W(s), \quad (8)$$

where the variable s represents the arc length of the ship trajectory. For the ship moving at a constant velocity v , the arc length at any time t is given by $s(t) = v \cdot t$. The variable ω_{dwc} is the dynamic width characteristic at that point on the trajectory corresponding to the arc length s .

By establishing the dynamic width characterization function for each sub-waterway unit and then combining them, the dynamic width characterization function for the entire waterway can be determined. This process is described in Algorithm 1.

Algorithm 1 Dynamic Width Characterization Function for Sub-waterway Units.

- 1: **Define:** geometric elements $H_i (i \in \{1, 2\})$, ship location $P(t) = [x(t), y(t)]^T$ and movement direction $\phi(t)$;
 - 2: **Initialize:** $t = 0$, $\Delta t = 1s$, $v = 1m/s$, $goal = [x_{end}, y_{end}]^T$, an empty list R ;
 - 3: **while** $dist(P(t), goal) > 0$ **do**
 - 4: Calculate $\frac{dD_{H_i}}{dt}$ according to (4)-(5);
 - 5: Calculate $w_{P(t)} = \min(D_{H_1}, D_{H_2})$;
 - 6: **if** $D_{H_1} < D_{H_2}$ **then**
 - 7: Calculate $\phi(t)$ such that $\frac{dD_{H_1}}{dt} = v$;
 - 8: **else if** $D_{H_1} > D_{H_2}$ **then**
 - 9: Calculate $\phi(t)$ such that $\frac{dD_{H_2}}{dt} = v$;
 - 10: **else**
 - 11: Calculate $\phi(t)$ such that $\frac{dD_{H_1}}{dt} = \frac{dD_{H_2}}{dt}$;
 - 12: Append $w_{P(t)}$ to the list R ;
 - 13: **end if**
 - 14: Update $P(t + \Delta t) \leftarrow P(t) + v \cdot \Delta t \cdot \begin{bmatrix} \cos(\phi(t)) \\ \sin(\phi(t)) \end{bmatrix}$;
 - 15: $t \leftarrow t + \Delta t$;
 - 16: **end while**
 - 17: **Return** the dynamic width characterization function based on R ;
-

3) *Waterway Intersection* : The intersection of an intricate waterway presents a special scenario when calculating dynamic width characteristics, as it involves more than two geometric boundaries. Consider the case of three intersecting waterways, as shown in Fig. 4. By following the previously mentioned calculation process, we identify a point P_a at the intersection. This point is equidistant from the upper,

lower, and right geometric boundaries, representing the largest minimum distance to these geometric boundaries. Using P_a as a reference, the waterway can be divided into three distinct sections.

More specifically, as the object moves from left to right through Waterway I, it continues calculating the dynamic width characterization function. Upon reaching P_a , the ship can enter either Waterway II or Waterway III. If it chooses Waterway II, the dynamic width characterization function is computed based on the upper and right boundaries. Similarly, the function for Waterway III can be determined. This is applicable to the intersections in both geographical contexts and those caused by traffic or other barriers (e.g., shallow waters, or buoys). By tracking the ship's movement and identifying points where it has more than two nearest geometric elements, it is possible to detect intersections and compute the dynamic width characterization function for complex, intersecting waterways effectively.

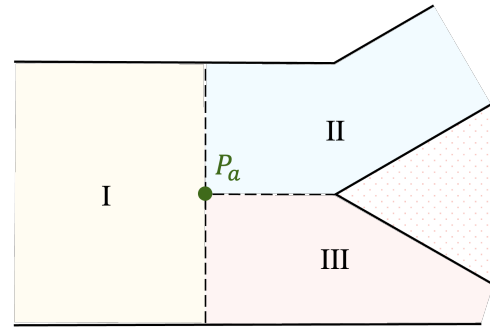


Fig. 4. Sketch of the Waterway Intersection Condition

III. SAFETY ROUTE DECISION

A. Geometric Analysis-based Route Safety Assessment

Based on the dynamic width characterization function, navigation safety assessments can be conducted to support route decision-making for ships. We propose the Geometric Analysis-based Route Safety Assessment (GARSA), which is applicable to narrow, rugged, and intricate waterway environments. By analyzing the geometric boundaries of irregular waterways, GARSA explores all feasible routes and establishes the corresponding dynamic width characterization functions. These functions describe the variation in waterway width along each route, providing a measure of navigational safety in terms of maneuvering space. To facilitate the selection of the safest route, a safety performance index is introduced, which converts the dynamic width characterization functions of each route into numerical scores for easy comparison. This process is detailed in Fig. 5.

1) *Calculation of Dynamic Width Characterization Function*: After appropriately simplifying the boundaries of irregular waterways, they can be abstractly represented using point and line features without losing generality. GARSA calculates the dynamic width characteristic by utilizing these point and line boundary features. This calculation can be seen as a process of object movement, where intersections and

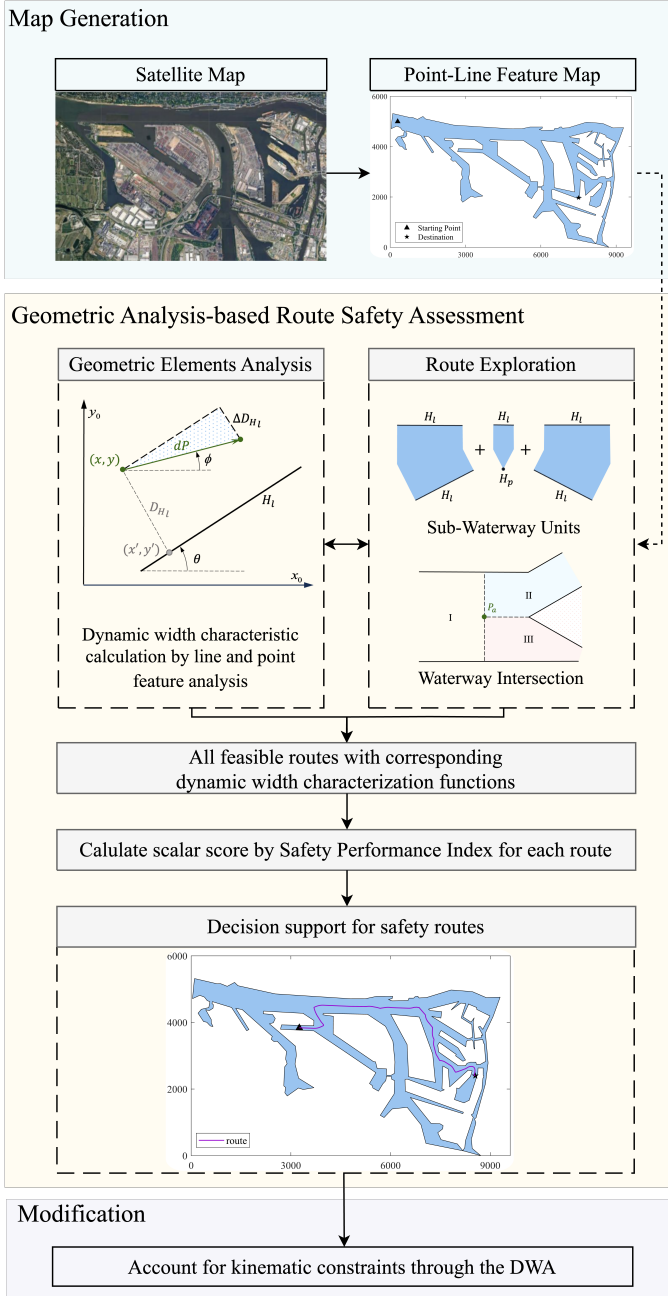


Fig. 5. Diagram of the Safety Route Decision Support Process

connectivity relationships of sub-waterway units are identified, as discussed in Section II. In this process, intersections are represented as nodes, and every branching path must be navigated. A pathway is fully explored once the object either reaches the terminus of the waterway or encounters a node that has already been explored. By traversing all sub-waterway units and intersections, the exploration of all possible routes can be conducted while establishing the corresponding dynamic width characterization function. The process of calculating the dynamic width characterization function for a feasible pathway is shown in Fig. 6.

2) *Safety Performance Index*: Based on the dynamic width characterization function of routes, the navigational safety

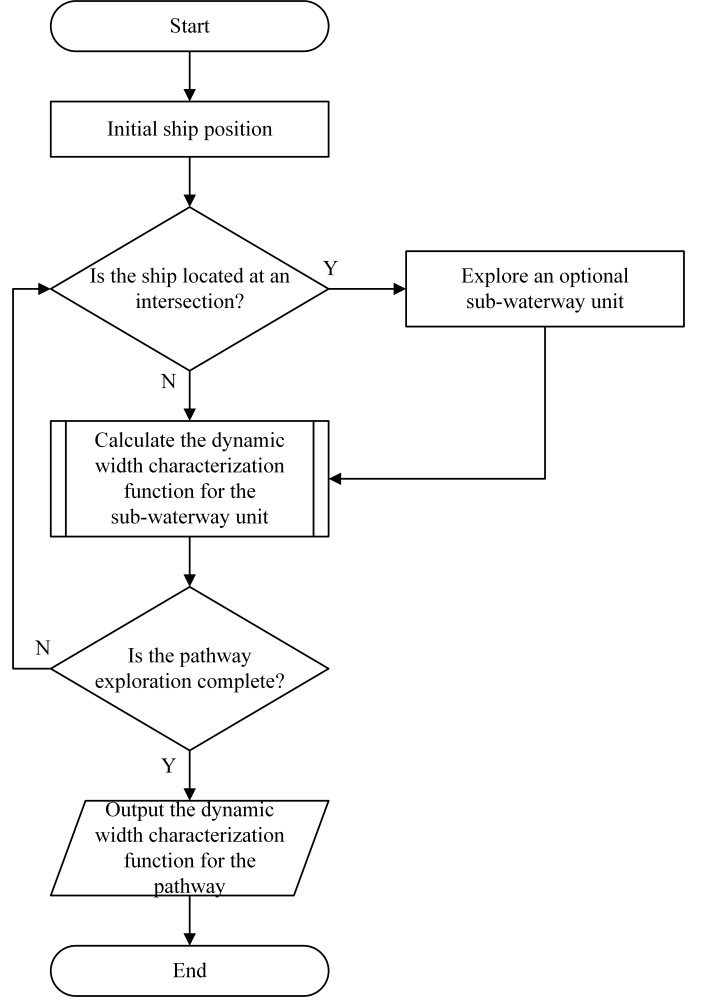


Fig. 6. Calculation Flowchart of Dynamic Width Characterization Function for a Pathway

can be assessed and reflected in a decision support system. Since comparing functions is complex, we propose a safety performance index (SPI) that converts the dynamic width characterization functions into numerical scores.

The SPI is constructed as a ratio, with the average waterway width of the entire route serving as the numerator and the risk associated with narrow sections acting as the denominator. Suppose the trajectory generated by the object is discretized into n points. The SPI is defined as

$$\kappa_{sp} = \frac{\bar{\omega}_{dwc}}{\sum_{i=1}^n -\log_{10}\left(\frac{W(s_i)}{\xi}\right) \cdot \mathbb{1}_{\{W(s_i) < \xi\}}}, \quad (9)$$

where $\bar{\omega}_{dwc}$ represents the average dynamic width characteristic along the trajectory. The function $\mathbb{1}$ is an indicator function, which equals 1 when the dynamic width characteristic $W(s_i)$ at point s_i is smaller than the threshold ξ , and zero otherwise.

This ratio-based formulation inherently balances global navigational safety and local risk. It means that a route with generally wide waterways but with some highly constrained sections will yield a lower index, highlighting the local risks even in globally safe waters. This property makes the index particularly useful for comparing different routes. For exam-

ple, For example, a route with a consistent, moderate width throughout may have a higher SPI than a route that features wide sections interspersed with narrow, risky areas.

By providing a quantifiable measure of navigational safety, this index aids in decision-making processes. It can guide autonomous ship in selecting safer routes, taking into account both overall route characteristics and localized risks. Additionally, it can also serve as a monitoring tool for navigational authorities, helping them implement safety measures in areas with lower SPI values due to narrow and intricate waterway sections.

B. Path Modification

The pathways generated by the GARSA method are derived from a geometric boundary analysis, representing feasible navigable routes, but they do not strictly correspond to tracked paths in the traditional sense. When the complex geometric boundaries are composed of numerous point and line elements, the generated pathways tend to have many twists and turns. To address this, we provide a path modification method based on the dynamic window approach (DWA) [29] to comprehensively consider the kinematic constraints of the ship [30], thereby producing a more navigable route.

DWA is a commonly used local path planning algorithm that takes into account the constraints of the ship's speed and acceleration. Its principle is as follows: within the allowable ranges for the ship's maximum speed and yaw rate, the algorithm computes multiple feasible paths over a time interval and selects the optimal path based on a thorough evaluation. In the comprehensive evaluation of feasible paths, DWA considers the distance between the ship and the destination, whether the ship's heading is aligned with the destination, and the distance between the ship and the shore.

In this research, the practical application method of DWA is as follows. Firstly, multiple waypoints are selected along the route generated by GARSA. Secondly, the DWA method is employed to plan paths reaching these waypoints one by one.

IV. EXPERIMENTS

To validate the effectiveness of the proposed method, the Port of Hamburg is utilized as the test environment. This waterway system is characterized by numerous intersections, intricate connectivity between sub-waterway units, and multiple narrow, rugged passages. The remote sensing map of the waterways (see Fig. 7(a)) is pre-processed into point-line feature maps (see Fig. 7(b)). On this basis, the route decision-making based on the proposed GARSA framework is tested and analyzed comprehensively.

Firstly, the route network modeling function is illustrated in subsection IV-A. Secondly, we explore the safety assessment capabilities for three scenarios in subsection IV-B, which include the entry port, exit port, and traversal within the port. Finally, in subsection IV-C, we test the path modification function and conduct a comparative experiment with the A* algorithm.

A. Route Network Modeling by Geometric Analysis

Fig. 7 shows a snapshot of the route exploration within the Port of Hamburg conducted by the GARSA framework. The exploration is carried out through the iterative calculations of object's movements, as described in Section II. This process provides an initial representation of all potential pathways within the waterway, while simultaneously capturing dynamic width characteristics.

Specifically, the exploration begins from an initial position, with a virtual MASS moving along the waterways while keeping as far as possible from nearby boundary geometric elements. In this process, intersections are treated as nodes, and all branches need to be traversed. A complete pathway is considered explored when the object either reaches the end of the waterway or encounters a previously explored node. Figs. 7(c) and 7(d) illustrate two sample pathways. Once all pathways have been explored, as shown in Fig. 7(e), we can filter the possible routes to a target point by identifying the pathway that connects the starting point to the target point. In this example, a total of 16 feasible routes are identified, traversing 8 intersections within the waterway system, as shown in Fig. 7(f). This process can be seen as an initial map representation process from the perspective of geometric analysis.

Fig. 7(g) presents the route network model, revealing the connectivity and spatial properties between the intersection nodes. The dynamic width characteristics are illustrated by a heat map along the connection pathways, where the color gradient from blue to red reflects the varying widths. Blue indicates wider sections, suggesting areas with potentially lower navigational risks and greater ease of transit. In contrast, darker red represents narrower, more constrained spaces that may pose higher navigational challenges or risks, thereby quantifying the variation in the width of the waterways. Consistent with the map visualization, the pathways between nodes 6 and 7, nodes 4 and 6, and from node 8 to the target exhibit narrower areas that require careful consideration. The extracted connectivity and width data provide valuable insights into the spatial dynamics of the waterway, supporting further risk assessment and decision-making in navigation planning.

B. Decision Support for Safety Routes

In this subsection, we explore the comprehensive decision-support capabilities of the GARSA method. The scenarios considered include port entry, port exit, and inter-port transit. Given a starting point and a target point, our objective is to explore potential routes and provide decision support for navigation safety. The process follows the steps shown in Fig. 5, including route exploration, the calculation of dynamic width characterization functions, and assessment using the safety performance index (SPI), with a set threshold of $\xi = 70$. Navigation zones recommended by conventions and rules are not considered in this subsection; instead, we use the geography of the Port of Hamburg as a test case to evaluate the performance of the proposed method. This assumption is acceptable, since we can further refine the point-line feature map by incorporating the existing navigation rules and zones.

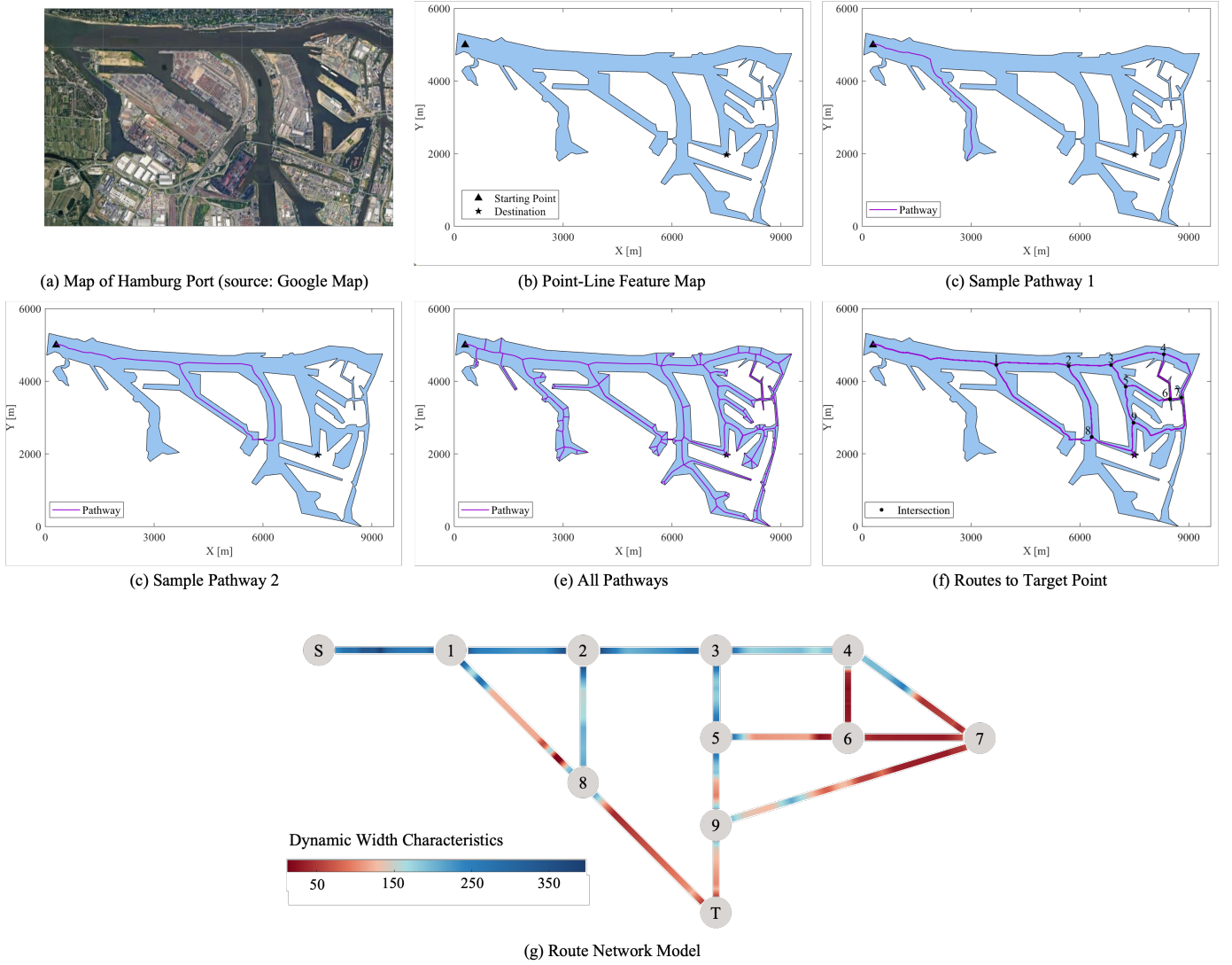


Fig. 7. Snapshots of Route Exploration in the Port of Hamburg

1) *Case 1: Port Entry*: Figs. 8(a)-(e) present five explored routes as illustrative examples. Intuitively, Routes 1 and 2 pass through the upper right region of the map, where narrower waterways increase the risk of collisions. This is a result of GARSA exploring all possible pathways. In contrast, Routes 3, 4, and 5 are depicted with better navigational safety, although Routes 3 and 4 also pass through several constricted areas. Fig. 8(f) presents the dynamic width characterization functions for Routes 3, 4, and 5, providing detailed insights into the relationship between route length and the varying widths along each route. Specifically, Route 3 encounters multiple narrow and potentially hazardous areas, with dynamic width measurements at the route lengths of 6,200, 6,600, and 7,300 meters being 64, 14, and 40 meters, respectively. In contrast, Route 4 exhibits a dynamic width of 40m at the 7800-meter mark, which aligns with the 7300-meter point on Route 3. Comparatively, Route 5 maintains a dynamic width greater than 70m throughout, ensuring a consistently safer navigational path up to the target point.

Using the safety performance index (SPI) formula in (9),

the navigational safety of each route is quantified, as shown in Table I. Route 5 emerges as the safest option with the highest SPI value. This finding aligns with the map visualization, which illustrates a favorable width profile and fewer narrow sections along the route. In contrast, Routes 1 and 2 exhibit the lowest SPI values, primarily because they traverse extended narrow areas. Although their average dynamic widths are acceptable, these constricted segments significantly degrade their overall safety performance. Route 3 also has a low SPI, despite having the shortest route length. This is attributed to its path through several extremely narrow areas, with a minimum dynamic width of only 14 meters. This illustrates that SPI is not influenced by route length. While Routes 4 and 5 have comparable average widths, Route 5's SPI is notably higher, reflecting the effectiveness of SPI in accounting for local narrow regions. This demonstrates the sensitivity of SPI as a tool for assessing navigational safety across different routes.

2) *Case 2: Port Exit*: We reversed the starting point and target point to carry out the port exit task. Since the positions of the two points remain unchanged, the results are identical

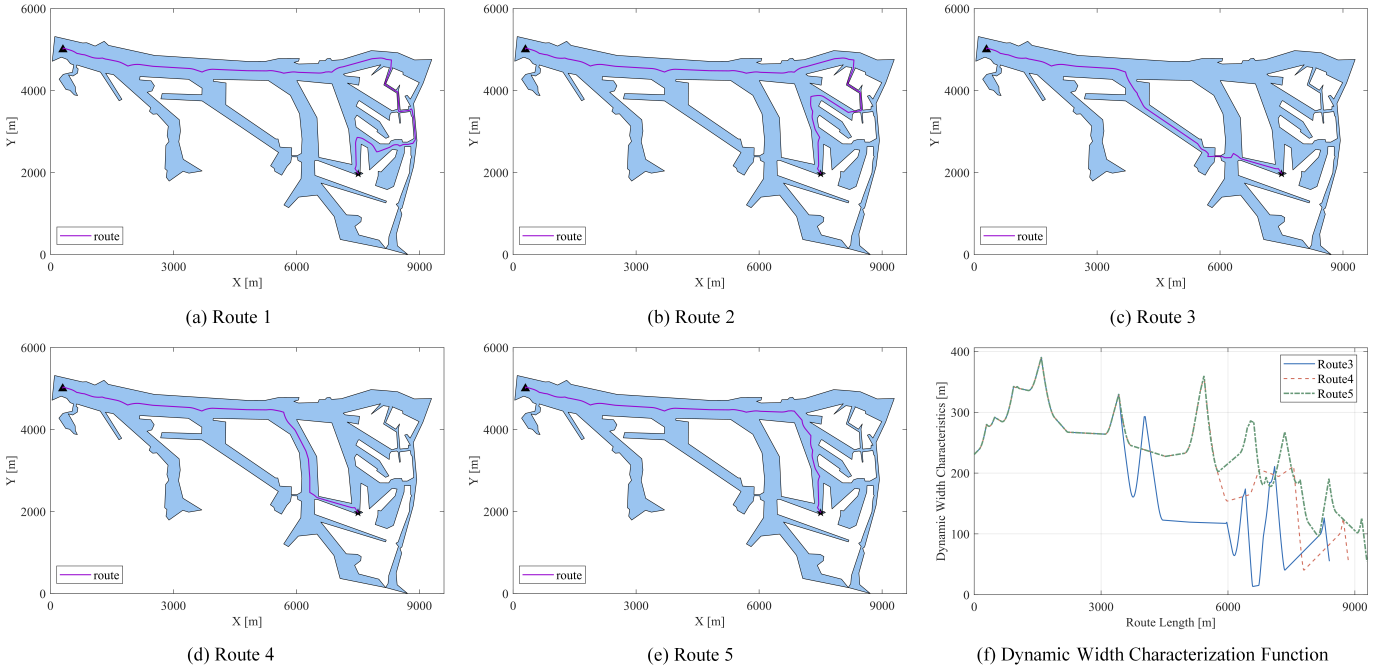


Fig. 8. Snapshots of Port Entry Route Exploration and Assessment

TABLE I

COMPARISON OF NAVIGATIONAL SAFETY ACROSS INBOUND ROUTES

Route Number	Mean DWC (m)	Minimum DWC (m)	Route Length (m)	SPI
1	188	18	13229	0.22
2	199	18	12865	0.33
3	194	14	8398	0.97
4	230	41	8848	4.07
5	240	55	9286	150.86

* DWC refers to the Dynamic Width Characteristic, SPI refers to Safety Performance Index.

to Case 1, demonstrating that Route 5 is the safest. This indicates that the proposed safety performance index (SPI) is independent of the direction of travel, relying solely on the geometric shape of the waterway.

3) *Case 3: Inter-port Transit*: Given the starting and target points illustrated in Fig. 9, the proposed GARSA framework explores 24 potential routes. Figs. 9(a)-(d) present four examples, Fig. 9(e) provides details of dynamic width characteristics, and Table II shows the safety assessment results using the SPI. Route 1, the narrowest with a mean dynamic width of 117 meters and a minimum dynamic width of 14 meters, has a low SPI of 0.59, indicating significant navigational challenges. While Routes 3 and 4 are similar in mean dynamic width and minimum dynamic width, both are significantly better than Route 1, Route 4's SPI of 135.10 is substantially higher than Route 3's SPI of 3.06. This discrepancy suggests that Route 3 may have some localized narrow areas compared to Route 4, consistent with the results from map visualizations, implying a balance of global navigational safety and local risk. Therefore, through the analysis of the GARSA framework, Route 4 is identified as the safest route.

Overall, the results demonstrate that the consistency of

TABLE II

COMPARISON OF NAVIGATIONAL SAFETY ACROSS INTER-PORT TRANSIT ROUTES

Route Number	Mean DWC (m)	Minimum DWC (m)	Route Length (m)	SPI
1	117	14	7258	0.59
2	161	14	10382	1.11
3	172	41	8956	3.06
4	195	50	7845	135.10

the GARSA framework in supporting safety route decision-making across various navigational tasks. The SPI offers a quantifiable and effective method for evaluating navigational safety, where higher scores are associated with wider routes and fewer narrow sections, providing intuitive insight into the relative safety of each route. By utilizing this approach, decision-makers can prioritize routes that minimize navigational risks, particularly in complex and constrained waterways like those found in the Port of Hamburg.

C. Path Modification and Comparative Experiment

Based on the Route 5 selected by GARSA in case of port entry, further modification is made using the dynamic window approach (DWA). During the application of DWA, multiple waypoints within Route 5 are selected, spaced at specific intervals, to allow DWA to plan paths sequentially to these waypoints. A comparative experiment between the modified route and a commonly used A* algorithm is conducted, as shown in Fig. 10. The A* algorithm, as a heuristic search method, aims to explore the optimal path length from the starting point to the target point. It uses the evaluation function comprised by the path cost from the initial state and the estimated cost of the shortest path to a goal state. After

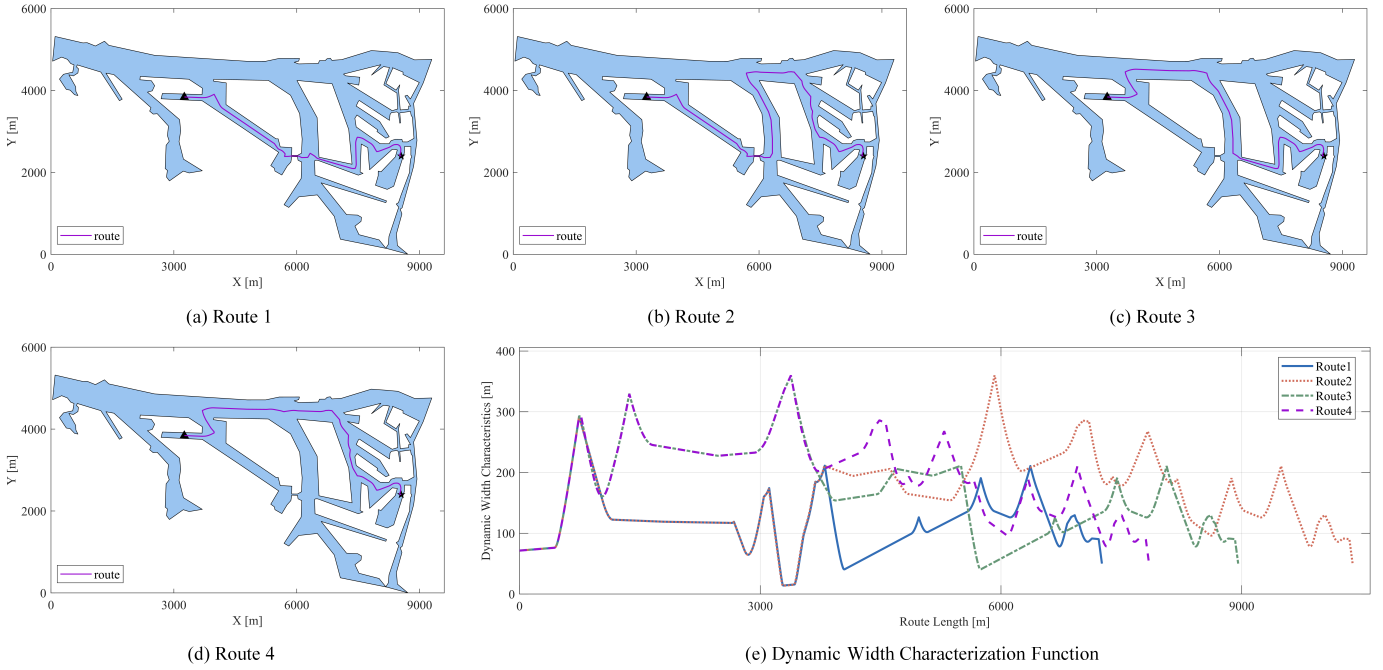


Fig. 9. Snapshots of Inter-port Transit Route Exploration and Assessment

performing gridding on the satellite map of the Hamburg harbor, the A* algorithm is applied to search the shortest path from the start to the destination. Our focus is on investigating the navigational safety of the waterways associated with the pathways generated by different methods. Therefore, the fact that the A* algorithm tends to produce routes close to the shoreline is not critical for our analysis and can be disregarded.

of path planning algorithms that may become trapped in narrow waterways.

V. SUMMARY

This paper presents the GARSAs method for route safety assessment in irregular waterways, prioritizing the safety issue in route decision-making for confined waters. Simulated experiments conducted in Hamburg Port validate GARSAs effectiveness in complex environments, leading to the following conclusions:

- 1) The GARSAs method effectively identifies safe pathways in narrow, rugged, and intricate waterways, reducing the risk of path planning algorithms making erroneous decisions in hazardous areas and enhancing the safety of autonomous ship navigation.
- 2) To measure navigational safety in irregular waterways, a dynamic width characterization function is developed based on geometric feature analysis. This function captures the dynamic spatial variations of complex channels, providing a basis for waterway capacity and safety assessments.
- 3) A safety performance index is proposed to support route decision-making. This index accounts for the average width of waterway along the entire route and the risks associated with locally narrow sections, facilitating the selection of the optimal and safest pathway.

The proposed method provides a foundation for advancing safe navigation in irregular waterways. Future work could explore real-world applications with varying environmental and operational constraints, expanding the method's adaptability to different geographic regions and vessel types.

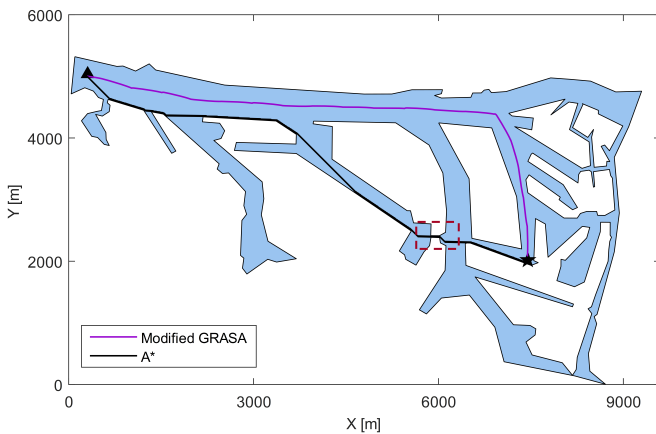


Fig. 10. Comparison Diagram of the Modified Safety Route and the Route Generated by A*

Although the A* algorithm selects a shorter route than the GARSAs method with the DWA modification, this shorter route passes through a narrow waterway approximately 30 meters wide and about 100 meters long, as indicated in the red-marked area in Fig. 10. This segment of the pathway significantly increases the collision risk for ships. This result demonstrates GARSAs effectiveness in assessing routes from a safety perspective, helping to avoid the hazardous decisions

REFERENCES

- [1] A. Bakdi and E. Vanem, "Fullest colregs evaluation using fuzzy logic for collaborative decision-making analysis of autonomous ships in complex situations," *IEEE Transactions on Intelligent Transportation Systems*, vol. 23, no. 10, pp. 18433–18445, Oct. 2022.
- [2] N. Forti, E. D'Afflisio, P. Braca *et al.*, "Next-gen intelligent situational awareness systems for maritime surveillance and autonomous navigation [point of view]," *Proceedings of the IEEE*, vol. 110, no. 10, pp. 1532–1537, Oct. 2022.
- [3] R. R. Negenborn, F. Goerlandt, T. A. Johansen *et al.*, "Autonomous ships are on the horizon: Here's what we need to know," *Nature*, vol. 615, no. 7950, pp. 30–33, Mar. 2023.
- [4] B. J. de Kruif, E. F. G. van Daalen, H. Cozijn *et al.*, "Control of a full port-to-port mission for a feeder vessel," in *OCEANS 2023 - Limerick*, Limerick, Ireland, 2023, doi: 10.1109/OCEANS2023.10244379.
- [5] G. Pedrielli, Y. Xing, J. H. Peh *et al.*, "A real time simulation optimization framework for vessel collision avoidance and the case of singapore strait," *IEEE Transactions on Intelligent Transportation Systems*, vol. 21, no. 3, pp. 1204–1215, Mar. 2020.
- [6] A. Haraldsen, M. S. Wiig, and K. Y. Pettersen, "A theoretical analysis of the velocity obstacle method for nonholonomic vehicles and underactuated surface vessels," *IEEE Transactions on Control Systems Technology*, vol. 32, no. 5, pp. 1801–1816, Sep. 2024.
- [7] X. Zhao, Y. He, L. Huang *et al.*, "Adaptive collision avoidance decision system for autonomous ship navigation," *Journal of Marine Engineering & Technology*, Dec. 2024.
- [8] R. Kandel and H. Baroud, "A data-driven risk assessment of arctic maritime incidents: Using machine learning to predict incident types and identify risk factors," *Reliability Engineering & System Safety*, vol. 243, Mar. 2024, art. no. 109779.
- [9] D. Nguyen, R. Vadaine, G. Hajduch *et al.*, "Geotracknet—a maritime anomaly detector using probabilistic neural network representation of ais tracks and a contrario detection," *IEEE Transactions on Intelligent Transportation Systems*, vol. 23, no. 6, pp. 5655–5667, Jun. 2022.
- [10] N. Wang, Y. Gao, C. Yang *et al.*, "Reinforcement learning-based finite-time tracking control of an unknown unmanned surface vehicle with input constraints," *Neurocomputing*, vol. 484, pp. 26–37, May. 2022.
- [11] K. Wakita, Y. Akimoto, D. M. Rachman *et al.*, "Collision probability reduction method for tracking control in automatic docking/berthing using reinforcement learning," *Journal of Marine Science and Technology*, vol. 28, no. 4, pp. 844–861, Dec. 2023.
- [12] L. Huang, C. Wan, Y. Wen *et al.*, "Generation and application of maritime route networks: Overview and future research directions," *IEEE Transactions on Intelligent Transportation Systems*, Nov. 2024.
- [13] J. Lee, W. Son, H. Lee *et al.*, "Verification of novel maritime route extraction using kernel density estimation analysis with automatic identification system data," *Journal of Marine Science and Engineering*, vol. 8, no. 5, May. 2020, art. no. 375.
- [14] X. Xu, B. Wu, J. Man *et al.*, "Bayesian network modelling for navigation status control of cargo ships in the three gorges waterway," *Reliability Engineering & System Safety*, vol. 245, Feb. 2024, art. no. 110018.
- [15] D. Jang and J. Kim, "Development of ship route-planning algorithm based on rapidly-exploring random tree (rrt*) using designated space," *Journal of Marine Science and Engineering*, vol. 10, no. 12, Dec. 2022, art. no. 1800.
- [16] C. Zhou, S. Gu, Y. Wen *et al.*, "Motion planning for an unmanned surface vehicle based on topological position maps," *Ocean Engineering*, vol. 198, Feb. 2020, art. no. 106798.
- [17] B. C. Shah and S. K. Gupta, "Long-distance path planning for unmanned surface vehicles in complex marine environment," *IEEE Journal of Oceanic Engineering*, vol. 45, no. 3, pp. 813–830, Jul. 2020.
- [18] M. Schoener, E. Coyle, and D. Thompson, "An anytime visibility-voronoi graph-search algorithm for generating robust and feasible unmanned surface vehicle paths," *Autonomous Robots*, vol. 46, no. 8, pp. 911–927, Dec. 2022.
- [19] X. Xin, K. Liu, S. Loughney *et al.*, "Multi-scale collision risk estimation for maritime traffic in complex port waters," *Reliability Engineering & System Safety*, vol. 240, p. art. no. 109554, 2023.
- [20] Y. Singh, S. Sharma, R. Sutton *et al.*, "A constrained a* approach towards optimal path planning for an unmanned surface vehicle in a maritime environment containing dynamic obstacles and ocean currents," *Ocean Engineering*, vol. 169, pp. 187–201, Dec. 2018.
- [21] S. Han, L. Wang, Y. Wang *et al.*, "A dynamically hybrid path planning for unmanned surface vehicles based on non-uniform theta* and improved dynamic windows approach," *Ocean Engineering*, vol. 257, Aug. 2022, art. no. 111655.
- [22] R. Song, Y. Liu, and R. Bucknall, "Smoothed a* algorithm for practical unmanned surface vehicle path planning," *Applied Ocean Research*, vol. 83, pp. 9–20, Feb. 2019.
- [23] S. Han, Y. Wang, L. Wang *et al.*, "Automatic berthing for an underactuated unmanned surface vehicle: A real-time motion planning approach," *Ocean Engineering*, vol. 235, Sep. 2021, art. no. 109352.
- [24] H. Li, W. Wang, H. Jiao *et al.*, "Bi-directional information fusion-driven deep network for ship trajectory prediction in intelligent transportation systems," *Transportation Research Part E: Logistics and Transportation Review*, vol. 192, p. art. no. 103770, 2024.
- [25] H. Li, W. Wang *et al.*, "Deep bi-directional information-empowered ship trajectory prediction for maritime autonomous surface ships," *Transportation Research Part E: Logistics and Transportation Review*, vol. 181, p. art. no. 103367, 2024.
- [26] L. Zhao, Y. Bai, and J. K. Paik, "Global-local hierarchical path planning scheme for unmanned surface vehicles under dynamically unforeseen environments," *Ocean Engineering*, vol. 280, Jul. 2023, art. no. 114750.
- [27] C. Liu, Q. Mao, X. Chu *et al.*, "An improved a-star algorithm considering water current, traffic separation and berthing for vessel path planning," *Applied Sciences*, vol. 9, no. 6, p. 1057, Mar. 2019.
- [28] Y. Wang, C. Lu, P. Wu *et al.*, "Path planning for unmanned surface vehicle based on improved q-learning algorithm," *Ocean Engineering*, vol. 292, Jan. 2024.
- [29] D. A. de Lima and A. C. Victorino, "A hybrid controller for vision-based navigation of autonomous vehicles in urban environments," *IEEE Transactions on Intelligent Transportation Systems*, vol. 17, no. 8, pp. 2310–2323, Aug. 2016.
- [30] T. I. Fossen, *Handbook of Marine Craft Hydrodynamics and Motion Control*, 2nd ed. Chichester, UK: John Wiley & Sons, Ltd., 2021.